Genome scale mutational analysis of *Geobacter sulfurreducens* reveals distinct molecular mechanisms for respiration of poised electrodes vs. Fe(III) oxides

Chi Ho Chan[a], Caleb E. Levar[a,b], Fernanda Jiménez-Otero[a,c], Daniel R. Bond[a,b,c]

BioTechnology Institute[a], Department of Microbiology[b], and Department of Biochemistry, Molecular Biology, and Biophysics[c], University of Minnesota-Twin Cities, Saint Paul MN 55108

Short title: Tn-Seq in *Geobacter*

Send all correspondence to:

Daniel R. Bond
140 Gortner Laboratory
1479 Gortner Ave
St. Paul, MN 55108
dbond@umn.edu

Keywords: *Geobacter*, extracellular electron transfer, Tn-Seq, multiheme cytochrome

Abstract

Geobacter sulfurreducens generates electricity by coupling intracellular oxidation of organic acids with electron transfer to the cell exterior, while maintaining a conductive connection to electrode surfaces. This unique ability has been attributed to the bacterium's capacity to also respire extracellular terminal electron acceptors that require contact, such as insoluble metal oxides. To expand the molecular understanding of electricity generation mechanisms, we constructed *Geobacter sulfurreducens* transposon mutant (Tn-Seq) libraries for growth with soluble fumarate or an electrode surface as the electron acceptor. Mutant libraries with over 33,000 unique transposon insertions and an average of 9 transposon insertions per kb allowed identification of 1,214 genomic features essential for growth with fumarate, including over 270 genes with one or more functional homologs that could not be resolved by previous annotation or *in silico* modeling. Tn-Seq analysis of electrode-grown cells identified mutations in over 50 genes encoding cytochromes, processing systems for proline-rich proteins, sensory systems, extracellular structures, polysaccharides, metabolic enzymes and hypothetical proteins that caused at least a 50% reduction in apparent growth rate. Scarless deletion mutants of genes identified via Tn-Seq revealed a new putative *c*-type cytochrome conduit complex (*extABCD*) essential for growth with electrodes, which was not required for Fe(III)-oxide reduction. In addition, mutants lacking components of a putative methyl-accepting chemotaxis/cyclic dinucleotide sensing network (*esnABCD*) were defective in electrode growth, but grew normally with Fe(III)-oxides. These results suggest that *G. sulfurreducens* possesses distinct mechanisms for recognition, colonization, and reduction of electrodes compared to other environmental electron acceptors.

76 **Importance**

77

78 Many metal-reducing organisms can also generate electricity at anodes. Because metal oxide
79 electron acceptors are insoluble, one hypothesis is that cells sense and reduce metal particles
80 using the same molecular mechanisms used to form biofilms on electrodes and produce
81 electricity. However, by simultaneously comparing thousands of *Geobacter sulfurreducens*
82 transposon mutants undergoing electrode-dependent respiration, we discovered new
83 cytochromes and chemosensory proteins essential for growth with electrodes that are not
84 required for metal respiration. This supports an emerging hypothesis where *G. sulfurreducens*
85 recognizes surfaces and forms conductive biofilms using sensing and electron transfer
86 pathways distinct from those used for growth with metal oxides. These findings provide a
87 molecular explanation for studies that correlate electricity generation on electrode surfaces with
88 direct interspecies electron transfer rather than metal reduction by *Geobacter* species, and
89 reveal many previously unrecognized targets for improving and engineering this
90 biotechnologically useful capability in other organisms.
91

Introduction

While most electron acceptors are soluble and easily reduced by inner membrane respiratory proteins, some electron acceptors are insoluble or lie beyond the cell surface. Bacteria able to catalyze 'extracellular electron transfer' or 'extracellular respiration' contain redox proteins and attachment mechanisms able to create electrical connections between membranes and these external substrates. Multiple modes of extracellular respiration are known, including reduction of Fe(III) and Mn(IV) oxides (1, 2), electricity production at electrode surfaces (3, 4), and formation of between-cell conductive networks enabling syntrophic growth with electron-consuming methanogens (5, 6).

The facultative anaerobe *Shewanella oneidensis* uses a single pathway comprised of the CymA inner membrane cytochrome and the MtrABC porin-multiheme *c*-type cytochrome complex to deliver electrons to all tested external metals and electrodes (7, 8). In contrast, there is evidence for multiple levels of complexity in the respiratory chain of the anaerobe *Geobacter sulfurreducens*. *G. sulfurreducens* requires two different inner membrane *c*-type cytochromes, ImcH and CbcL, depending on the reduction potential of the extracellular acceptor (9, 10). Up to five homologs of the PpcA periplasmic tri-heme *c*-type cytochrome could be involved in assisting electron transfer across the periplasm (11). To cross the outer membrane, one electron transfer 'conduit' complex consisting of the OmaB multiheme *c*-type cytochrome, OmbB porin-like protein, and OmcB multiheme lipoprotein *c*-type cytochrome is essential for growth with some metals (12, 13), but the genome encodes at least five other putative porin-cytochrome complexes with unknown functions. At the outer surface, *Geobacter* must build a conductive interface to reach metal particles, electrode surfaces, or partner bacteria. Simple extracellular polysaccharides influence biofilm interactions (14), while a combination of conductive Type IV pili and multiheme *c*-type cytochromes such as OmcS, OmcE, OmcZ and

PgcA are implicated in electron transfer beyond the cell membrane, depending on growth conditions (12, 14–16).

Due to the ease of screening mutants in liquid medium, compared to growth on electrodes in electrochemical reactors, most components of the *Geobacter* electron transfer pathway are identified using metals as proxies for other extracellular acceptors (14). Transposon-based mutagenesis using metals has revealed crucial cytochromes and attachment strategies, but high-throughput colorimetric screens are designed to identify mutants with growth rates near zero. Unfortunately, as multiple overlapping electron transfer pathways exist and many electron transfer proteins have functional homologs, single mutations typically decrease rather than eliminate growth of *G. sulfurreducens* (17, 18). This respiratory complexity, combined with the bottleneck of studying electron transfer in electrode biofilms, severely limits the pace of discovery when studying the molecular basis of complex phenotypes such as electricity production.

Transposon-insertion sequencing, also known as Tn-Seq, is able to quantify the abundance of every mutant containing a transposon insertion within a library, without individual mutant isolation (19). Using Tn-Seq, it is possible to measure the effect every mutation has on growth rate, by comparing an insertion's abundance before and after a known number of generations. This method rapidly assessed gene essentiality under aerobic versus anaerobic growth in *Shewanella oneidensis*, revealed genes essential to different respiration strategies in *Rhodopseudomonas palustris,* and uncovered the essential gene set in the archaeon *Methanococcus maripaludis* (20–22). For this report, we constructed the first *G. sulfurreducens* Tn-Seq library, and used it to define over 1,200 genes essential for growth in minimal medium using a soluble electron acceptor. By then cultivating this same mutant library on electrode surfaces, a subset of over 50 additional genes that caused at least a 50% decrease in growth

rate was revealed. Surprisingly, mutants lacking these new key cytochromes or chemosensory genes were severely impaired in growth with electrodes, but remained fully able to respire using other extracellular metal acceptors. These results suggest that separate biochemical mechanisms are used for electron transfer to electrodes and to environmental metals.

Results and discussion

Tn-Seq in *G. sulfurreducens*. *G. sulfurreducens* transposon libraries were generated using a *mariner*-based transposon with directional type IIS MmeI recognition sites engineered on both ends of the transposon insertion sequence (22, 23). As MmeI cleaves chromosomal DNA 20 base pairs from its recognition site, adapter ligation and amplification allows sequencing to identify most insertions and quantify each mutant's abundance (24). After three separate transposon libraries were constructed using fumarate as the electron acceptor, approximately 50,000 individual colonies were recovered per library, and sequencing revealed between 30,000 and 33,000 independent insertions in each library with no obvious hotspots or biases in coverage. The library representing the deepest coverage was used as the source for all experiments reported in this work.

When DNA from two separate cultures within the same library was extracted, digested with MmeI, ligated to Illumina adaptors, amplified, and sequenced, 33,257 and 33,343 unique insertions were identified in the two replicates. Over 97% of insertions occurred within annotated features at an average density of 9 unique insertions per kb (25). Despite opportunities for bottlenecking and bias during each growth, extraction, labeling and sequencing step, the number of reads mapped per annotated feature was reproducible with a Pearson's coefficient of 0.98 between the two culture replicates (Fig. 1A). When two independent cultures were further grown with poised electrodes as the electron acceptor, then separately recovered, extracted,

and labeled, the number of reads mapped per gene in each independent growth experiment was similarly reproducible with a Pearson's coefficient of 0.98 (Fig. 1B).

Essential genes for growth using fumarate in *G. sulfurreducens.* To predict genes important for growth with electrodes, genes required for growth in standard minimal medium with the electron acceptor fumarate were first determined, so they could be excluded from further analyses. Tn-Seq libraries were grown in liquid culture for 6 generations and sequenced to a depth of >40 M reads per culture replicate. At this depth, an average of 1,200 reads are obtained per insertion, and based on an average feature size in *G. sulfurreducens* of 0.95 kb/feature, 10,200 reads are expected to map to each feature in the annotated genome.

Previous constraint-based modeling predicted that a set of 140 central metabolic and biosynthetic genes should be essential for growth using fumarate as the sole electron acceptor (26). The majority (>90%) of these predicted essential genes had less than 300 mapped reads in our Tn-Seq analysis, compared to an expected 10,200 reads/gene, or they contained less than 4 insertions per kb (Fig. 2, Table S2). A small subset of genes previously predicted to be essential *in silico* averaged over 8,100 reads/feature and 10 insertions per kb, similar to other non-essential genome regions, and were considered to be non-essential under our growth conditions. Based on these results, annotated features with less than 300 reads mapped per feature or 4 insertion sites per kb were categorized as essential. Using both criteria allowed correction for small genes with few transposon insertion sites (TA dinucleotide) as well as larger genes which can support insertions between domains (27). According to this cutoff, over 170 genes previously coded as non-essential in the *in silico* model were essential in our minimal medium. Most of these encoded biosynthetic pathways for biotin, riboflavin, and cobamide, as our medium lacked vitamins. In addition, biosynthesis pathways for heme, fatty acids, and lipopolysaccharides, along with putative transporters for sulfate, acetate, copper, cobalt, and

197 magnesium were essential. Complete tables comparing *in silico* predictions with Tn-Seq results
198 are in Tables S3-S4.
199
200 In total, almost 40% of annotated features, or 1,214 genome features out of 3,706, were
201 identified as essential for growth with acetate as the electron donor and fumarate as the sole
202 electron acceptor. A key difficulty in the original *G. sulfurreducens* annotation and *in silico*
203 metabolic model was that genes encoding homologs or redundant pathways were not assigned
204 function, as they could possibly complement each other (18, 19). Tn-Seq analysis clarified
205 hundreds of such issues. For example, despite the presence of five annotated ferredoxins, only
206 one was essential (GSU2708), one of three 2-oxoglutarate dehydrogenase complexes was
207 essential (GSU1467 – GSU1470), one of three aconitase enzymes was essential (GSU1660),
208 one of two fructose bisphosphate aldolases was essential (GSU1193), and two of three
209 phosphoglycerate mutase enzymes were essential (GSU1818 and GSU3207). In total, Tn-seq
210 resolved the essentiality of over 270 such examples where homologs were present but only
211 specific genes were required under laboratory conditions (Table S5-S6).
212
213 Of special interest in *Geobacter* electron transfer is the mechanism of NADH oxidation and
214 electron delivery to the quinone pool. This remains poorly understood, partially due to the fact
215 that most *Geobacteraceae* encode two distinct complex I-NADH dehydrogenases (28). The
216 complex I similar to that found in other Proteobacteria, recently classified as type “E” (GSU3429
217 – GSU3445) was not essential in *G. sulfurreducens*. However, a second, less well characterized
218 complex I was essential. This NADH dehydrogenase does not fall into a major defined clade,
219 and is most closely related to complex I sequences in *Chloroflexi* (GSU0338 – GSU0351) (28).
220 A second essential gene cluster with bioenergetic implications was an integral membrane *b*-type
221 cytochrome/FeS cluster/electron transfer flavoprotein. These genes (GSU2795 – GSU2797)
222 encode all signature residues of confurcation/bifurcation complexes, suggesting high and low

223 potential electrons (such as NADH + reduced Fd) may be combined for quinone pool reduction
224 or proton translocation events during oxidation of acetate (29).
225
226 **Genes affecting electrode growth of *G. sulfurreducens*.** Growth on an electrode surface in
227 microbial fuel cells and electrochemical devices is hypothesized to be a complex phenotype that
228 requires attachment, movement of electrons across membranes, and formation of between-cell
229 conductivity to sustain respiration by cells not in contact with the surface (9, 10, 14, 30, 31). To
230 test the entire process from attachment to biofilm growth, two parallel Tn-Seq libraries were
231 grown for 6 generations on an electrode poised at -0.1 V vs. Standard Hydrogen Electrode
232 (SHE), and the density of reads mapped per feature compared to parallel fumarate-grown cells.
233 The electrode potential (-0.1 V vs. SHE) was chosen to mimic the redox potential of
234 environmental Fe(III) oxides (32).
235
236 Expressing Tn-Seq read density data as Log_2 ratios allows quick assessment of a phenotype.
237 For example, a mutation preventing growth in a mutant results in twice as many wild type reads
238 after one generation, or a Log_2 ratio of -1. Using the exponential growth equation, genes with a
239 Log_2 score of -2 after 6 generations are equivalent to at least a 50% reduction in apparent
240 doubling time. Using this criteria, nearly 50 genes encoding cytochromes, protein processing
241 systems, sensing proteins, extracellular structures, polysaccharides, metabolic enzymes and
242 hypothetical proteins were involved in electrode growth. Full data showing all read mapping
243 densities and Log_2 ratios for all features is in Table S2, and all raw read data needed to re-
244 create this analysis is available in NCBI BioProject PRJNA290373. Direct links for downloading
245 read mapping files and the annotated genome for viewing in IGV is in file S7.
246
247 Tn-Seq analysis confirmed a previous finding that CbcL, an inner membrane putative quinone
248 oxioreductase containing both *b*- and *c*-type cytochromes (GSU0274) is crucial for electrode

249 growth when electrodes are poised at -0.1 V vs. SHE (9, 10). Insertions in *cbcL* resulted in Log_2
250 ratios corresponding to doubling times of 17.4 h, while a ~20 h doubling time was previously
251 estimated for a pure culture Δ*cbcL* mutant (9). Also in agreement with previous work was the
252 severe negative impact of insertions in genes involved in assembly and expression of the
253 conductive Type VI pili. Insertions in the *pilQPOM* operon (GSU2028 – GSU2032), *pilC* gene
254 (GSU1493) and *pilS* sensor kinase (GSU1494) produced similar defects, while insertions in
255 other Type VI pili genes predicted weaker phenotypes (below the threshold in Table 2), but still
256 causing at least a 25% decrease in apparent growth rate. Insertions in some pili genes, such as
257 the *pilT4* gene (GSU1492), led to increased apparent abundance, consistent with recent reports
258 that pilT mutants more rapidly colonize electrodes (33).
259
260 Surprisingly, with the exception of CbcL, no other cytochromes reported to play a role in
261 electron transfer to metals appeared to be required for growth with an electrode in the Tn-Seq
262 analysis. Instead, insertions in two uncharacterized multiheme *c*-type cytochromes did
263 significantly affect electrode growth (GSU2643 and GSU2645). These cytochromes are part of a
264 cluster containing two multiheme *c*-type cytochromes, a multiheme lipoprotein cytochrome, and
265 a predicted outer membrane porin-like protein. As a similar arrangement of multiheme
266 cytochromes, lipoprotein cytochromes, and putative β-barrel proteins encodes a “conduit” for
267 electron transfer across the outer membrane in both *Geobacter* (the OmcB-based conduit) and
268 *Shewanella* (the MtrCAB conduit), this region was targeted for further study.
269
270 The *G. sulfurreducens* genome encodes over 100 histidine kinases, response regulators and
271 chemotaxis-like proteins, yet little is known about their role controlling phenotypes such as
272 extracellular respiration (34). Tn-Seq identified one DNA-binding protein (GSU0013), and four
273 chemotaxis proteins (GSU1704 and GSU2220 – GSU2222) as significant at the level of a 50%
274 growth reduction. Only one diguanylate cyclase-response regulator protein was suggested to

participate in electrode-dependent growth (GSU3376) above the level of a 25% reduction in growth. In model systems, methyl-accepting chemotaxis proteins such as GSU1704 undergo a conformational change to interact with CheW (GSU2220) and CheA (GSU2222) family proteins, triggering phosphorylation of GSU3376-like response regulators (35). Based on the hypothesis that GSU1704, GSU2220, GSU2222 and GSU3376 represented portions of MCP-CheA-CheW-response regulator systems involving the biofilm regulator c-di-GMP, these were also targeted for further study.

Some of the strongest phenotypes in apparent electrode growth were due to insertions in genes encoding sugar and polysaccharide synthesis. Five different sugar dehydrogenases, sugar transferases, and isomerases were identified as being required for electrode growth via Tn-Seq, and insertions within at least three different gene clusters involved in capsule, lipopolysaccharide and extracellular sugar synthesis produced significant defects. Also crucial were genes putatively involved in translocating sugars to the outer surface, such as a sugar ABC transporter previously shown to be essential for electrode growth (*xapD*, GSU1501), and an LPS ABC transporter protein (*lptA*, GSU1889). The defects created by these insertions further support a role for sugars in creating a properly charged or modified outer surface during *Geobacter* biofilm formation on electrodes (14, 16).

Finally, proteins involved in translation and processing of proline-rich proteins became important during electrode growth. For example, elongation factor P is essential for overcoming ribosome stalling during translation of proline-repeat sequences, and contributes to outer membrane integrity in *E. coli* (36, 37). Tn-Seq analysis predicted that one of two Ef-P homologs in *G. sulfurreducens*, (Efp-2, GSU1752), along with the Ef-P modifying Ef-P lysine-lysyltransferase (GSU1753) and Ef-P lysyl-lysine 2,3-aminomutase (GSU1754) became important during growth with electrodes. Insertions in a prolidase involved in cleaving peptides at proline residues (GSU

1105) and peptidylprolyl cis-trans isomerase (GSU2074) showed strong growth defects, further suggesting an unrecognized importance in the folding and processing of proline-rich proteins under electrode respiring conditions.

Possible genes missed by the community aspect of Tn-Seq analysis. Deletion of the outer surface cytochrome gene *omcZ* (GSU2076) can significantly decrease electrode growth (38). While Tn-Seq insertions in genes within the *omcZ* operon had a negative impact (such as the peptidylprolyl cis-trans isomerase, GSU2074), insertions in *omcZ per se* were not identified as causing a defect in our library experiments (38, 39). Similarly, the pili-associated cytochrome OmcS is reported to be involved in electron transfer to electrodes, yet it was not identified in our analysis. Both of these cytochromes are verified to exist beyond the cell membrane, in the conductive matrix between cells (39, 40).

Under Tn-Seq conditions, enzymatic activities and proteins can be shared. A clear example of population-based complementation was evident in Tn-Seq data for fumarate hydratase, a TCA cycle gene predicted *in silico* to be absolutely essential (GSU0944, Table S3). Due to the fact that wild type *G. sulfurreducens* secretes malate when grown with fumarate as the electron acceptor (41), we hypothesized that fumarate hydratase was not required by the small subpopulation of fumarate hydratase mutants, as extracellular malate can rescue the gap in the TCA cycle. Consistent with this hypothesis, during growth with an electrode in the absence of fumarate, fumarate hydratase became one of the most essential genes in Tn-Seq analysis.

Our data suggest that extracellular cytochromes such as OmcZ secreted by wild type cells may similarly aid the occasional Δ*omcZ* mutant in the biofilm population during Tn-Seq experiments. This phenomenon would be similar to how outer membrane proteins shared between *Myxococcus* strains rescue motility mutants (42), and siderophores act as “public goods” for

rare non-producing strains (43). In contrast to evidence that OmcS and OmcZ might be shared between cells, cellular machinery such as the Type IV pili, inner membrane cytochromes and outer membrane cytochromes remained essential even in biofilm conditions. Further Tn-Seq experiments may provide a mechanism to discover which *Geobacter* extracellular proteins can be shared for communal conductivity and exploited by 'cheaters' embedded in a conductive matrix, vs. which proteins catalyze key attachment or electron escape reactions so essential to each cell that they cannot be borrowed from neighbors.

Cytochrome conduit deletion mutants affect electrode- but not Fe(III)-reduction. While Tn-Seq agreed with the importance of previously reported mechanisms such as pili, inner membrane cytochromes, and extracellular sugars, it identified many processes never highlighted in any mutant, proteomic, or transcriptional study. Based on their strong phenotypes under Tn-Seq conditions, we investigated the roles of two surprising classes of mutants, involving new outer membrane cytochromes and signaling proteins, after constructing scarless deletions of these key genes and gene clusters.

In Tn-Seq data, no effect was observed for mutations in one of the most studied outer membrane *c*-type cytochromes in *G. sulfurreducens,* OmcB. Part of a trans-outer membrane porin-cytochrome conduit capable of transferring electrons across the outer membrane, OmcB is encoded in a three-gene cytochrome/porin-like protein/lipoprotein cytochrome cluster (*ombB-omaB-omcB,* GSU2737–GSU2739) located next to a nearly identical tandem duplication containing another conduit (*ombC-omaC-omcC,* GSU2731–GSU2733). This duplication limits the impact of single mutations in any one gene. Thus, a scarless deletion of this entire genomic region, lacking all genes in the *omcB* and *omcC*-encoded conduits was constructed, and is referred to here as Δ*omcBC* (ΔGSU2739 – GSU2731). Genes for a new putative porin-cytochrome conduit, that shares no homology with the OmcB or OmcC conduits, showed a

353 strong phenotype in Tn-Seq data. This conduit was termed *extABCD* (extracellular electron
354 transfer) and genes were removed to generate the ∆*extABCD* (ΔGSU2645-GSU2642) strain. In
355 addition, deletion mutants of two other putative outer membrane conduit clusters, Δ*extEFG*
356 (GSU2726 – GSU2724) and Δ*extHIJKL* (GSU2940 – GSU2936) were constructed as controls to
357 compare with Tn-Seq results.
358
359 The Δ*extABCD* strain grew poorly when the electrode was the electron acceptor, never
360 producing more than 50 μA/cm^2 when grown under the same conditions used for Tn-Seq. In
361 contrast, the Δ*omcBC* deletion strain showed no defect, and grew on the electrode similar to
362 wild type (Fig. 3A). The other mutants lacking outer membrane conduits, ∆*extEFG* and
363 ∆*extHIJKL,* also showed no defects on the electrode, demonstrating similar growth rates and
364 final current densities as wild type. All mutants grew with wild type growth rates using fumarate
365 as the electron acceptor, as predicted by Tn-Seq essentiality data (data not shown). While
366 single-gene replacement mutants lacking the *omcB* gene will grow in microbial fuel cells (44),
367 these results demonstrated that no part of the *ombB-omaB-omcB* and/or *ombC-omaC-omcC*
368 conduit genes were required for wild type colonization and reduction of electrodes. Two other
369 putative trans-outer membrane conduit gene clusters are also not essential for electron transfer
370 to electrodes. In both Tn-Seq and in pure culture studies with reconstructed mutants, only the
371 deletion of *extABCD* had any effect when electrodes were the electron acceptor.
372
373 In contrast to the strong electrode phenotype observed for the mutant lacking *extABCD*,
374 reduction of insoluble Fe(III)-oxide by Δ*extABCD* was unaffected. Even though metal oxide
375 particles are surfaces with similar redox potentials as the electrodes used in the Tn-Seq
376 analysis, the *extABCD* gene cluster was not essential for reduction of metals (Fig. 3B). The
377 phenotype of the Δ*extABCD* mutant suggests that the dominant pathway of electron transfer

across the outer membrane will vary, based on what is being used as the extracellular electron acceptor.

Chemosensory system deletion mutants also affect electrode- but not Fe(III)-reduction. A second class of genes revealed by Tn-Seq analysis were related to intracellular sensing and signaling systems. Based on their Tn-Seq phenotypes, these proteins were termed part of an electrode sensing network, and included; EsnA, a methyl-accepting chemotaxis protein (GSU1704), EnsB, a CheW-like chemotaxis scaffolding protein (GSU2220), EsnC, a CheA-like chemotaxis histidine kinase (GSU2222), and EsnD, a diguanylate cyclase (GSU3376). Scarless deletion mutants of each *esn* gene were constructed and tested for growth using an electrode as the electron acceptor.

All four *esn* deletion mutants displayed defects in growth with an electrode even more severe than the Log_2 ratios observed in Tn-Seq data (Fig. 3A and Table 2). However, when these same four *esn* mutants were grown with Fe(III)-oxide as the electron acceptor, Fe(III) reduction was similar to wild type (Fig. 3B). All mutants also grew at wild type growth rates with fumarate as the electron acceptor. This phenotype, where a mutant performed poorly with an electrode surface but still reduced metal oxide particles, agreed with the hypothesis that cells interact with these two solid-phase electron acceptors via different molecular mechanisms.

Further work will be required to determine if the similar phenotypes displayed by *esn*-encoded proteins is due to direct physical interactions or common signaling molecules. No annotated MCP genes in the *G. sulfurreducens* genome are co-localized in operons with a complete set of CheA-CheW genes, and no protein-protein interaction data is available to predict the downstream target of the EsnC CheA-like kinase. The EsnA methyl-accepting chemotaxis protein has no periplasmic sensing domain to suggest an external input for this system, but

404 EsnA does contain a cytoplasmic GAF domain typically involved in binding small molecules
405 such as cyclic nucleotides, and EsnD is a demonstrated cyclic-di-GMP producing response
406 regulator (45). One hypothesis is that EsnABC together regulates and/or responds to levels of
407 EsnD-produced cyclic-di-GMP, driving and reinforcing a switch to the conductive biofilm mode
408 of growth (46). Whatever the ultimate signal is for electrode colonization, it does not appear to
409 be involved in growth with metals such as Fe(III).
410
411 **Conclusions and outlook.** The ability of Tn-Seq to survey mutants across the entire genome in
412 a single growth experiment is especially useful when no high-throughput assay is available for
413 the phenotype under study. In the case of growth on electrodes, testing 33,000 individual
414 mutants in replicate electrode reactors would require our laboratory to dedicate its bank of 45
415 electrochemical cells to testing mutants nonstop for over 28 years. In a fraction of that time,
416 saturation mutagenesis described over 1,200 genes essential for growth under laboratory
417 conditions, resolved hundreds of annotation issues, and brought into focus over 50 genes vital
418 during electrode growth conditions.
419
420 By asking what genes are required for growth, Tn-Seq generates data different from expression-
421 based approaches which operate under the hypothesis that important genes will be strongly
422 regulated in response to an electrode. Transcriptional data did lead to discovery of the key
423 multiheme cytochrome OmcZ in *Geobacter*, and supported early hypotheses suggesting a role
424 for pili. However, microarrays also found strong up-regulation of many genes which failed to
425 show importance in follow-up mutant studies, and failed to show phenotypes in these Tn-Seq
426 results (38). Examples include; the OmcB and OmcC cytochromes and multiple hypothetical
427 cytochromes, amino acid transporters and hydrogenases, terminal oxidases involved in oxygen
428 reduction, and heavy metal exporters. In general, we found little overlap between genes
429 predicted as important to growth on electrodes via Tn-Seq and those up- or down-regulated in

430 expression or proteomic studies on electrodes (31, 38, 47). One possibility is crucial regulatory
431 or biosynthetic elements have low basal expression levels. Expression or abundance-based
432 studies could have reduced sensitivity if biofilms are heterogeneous, or if expression varies with
433 distance from the electrode (48). In the case of cytochromes, the *imcH* and *cbcL*-encoded
434 cytochromes involved in electron transport are now known to be expressed even when cells are
435 grown with fumarate, preventing their earlier discovery via differential expression (9, 10). It also
436 remains possible that electrodes, being relatively unnatural substrates, trigger additional
437 transcriptional changes or de-repress genes that have little to do with electrode respiration.
438
439 Tn-Seq data provided genome-scale information that agreed with prior *in silico* predictions and
440 knockouts during fumarate reduction (26, 49). However, much less data are available for
441 electrodes in terms of what genes are essential, and as with any large-scale survey,
442 reconstruction of mutants is needed to corroborate findings. Using scarless mutants lacking
443 genes and whole gene clusters, we were able to confirm that individual chemosensory
444 components of *esnABCD* and the entire cytochrome conduit *extABCD* were essential for growth
445 when the electrode acted as the electron acceptor. As two other outer membrane conduits,
446 based on OmcB and OmcC, are well-studied and known to be involved in electron transfer to
447 metals, we also constructed new mutants lacking these non-homologous cytochrome clusters,
448 along with two other unstudied putative outer membrane conduits. Surprisingly, only removal of
449 the *extABCD* conduit gene cluster affected electrode growth, as predicted by Tn-Seq.
450
451 When Fe(III) was the electron acceptor, none of the cytochrome conduit mutants with electrode
452 phenotypes, and none of the mutants lacking methyl-accepting chemotaxis proteins or GGDEF-
453 domain response regulators, had significant defects (Fig. 3B). These data support a model that
454 *G. sulfurreducens* possesses separate mechanisms for reduction of electrodes compared to the
455 reduction of metals that involves a distinct set of cytochromes for crossing the outer membrane.

456 In addition, separate cyclic dinucleotide-dependent regulatory systems may be used for
457 recognition and respiration of electrodes compared to metals.
458
459 A recent comparison of seven *Geobacter* species noted a poor correlation between electricity
460 production and Fe(III) reduction rates (50). In contrast, strains capable of high rates of electricity
461 production were also capable of interspecies electron transfer to methanogens. This correlation
462 led to the hypothesis that the conductive network accessible to electrodes evolved to support
463 direct electron transfer between *Geobacter* and electron-accepting organisms such as
464 methanogens. Evidence for this hypothesis lies also in the use of anaerobic digesters as the
465 most common source of high current-producing *Geobacter* enrichments (51), compared to
466 Fe(III)-rich environments (50, 52). A syntrophic partner may be much like an electrode; it can
467 accept electrons indefinitely, but requires commitment to an attached biofilm lifestyle and the
468 expense of building a conductive extracellular space (6, 53). In contrast, small metal oxide
469 particles represent a temporary and more variable electron acceptor, where cells cannot attach
470 permanently or grow into thick biofilms that entrap and re-use extracellular proteins (54).
471
472 While naturally-occurring *Geobacter* strains produce >1 mA/cm^2 of electrical current, and this
473 rate already rivals the best artificial enzyme-functionalized electrodes (55), use of microbial
474 electrochemistry as an energy source or biocatalyst is estimated to require at least a 10-fold
475 increase in current density in order to be profitable (56–58). Achieving these gains, and
476 engineering these abilities into industrial bacteria, requires identification and enhancement of
477 core components specific to electricity production. While the molecular basis for this
478 extracellular respiration is becoming more clear, how organisms biochemically distinguish
479 between insoluble metals vs. microbial or electrode-based acceptors remains a key challenge.

Materials and Methods

Growth and medium conditions. All strains and plasmids used in this study are listed in Table 1. *G. sulfurreducens* strains and mutants were grown from single colony picks streaked from lab DMSO stocks in anoxic basal medium as described (59). For routine growth, basal medium with acetate (20 mM) as the electron donor and fumarate (40 mM) as the electron acceptor was used. Agar (1.5%) was added to the acetate-fumarate medium when culturing for clonal isolates on semisolid surface in an H_2:CO_2:N_2 (5:20:75) atmosphere in a vinyl anaerobic chamber (Coy) or an anaerobic workstation 500 (Don Whitley). When electrodes were used as the electron acceptor, fumarate was replaced with 50 mM NaCl to maintain a similar ionic strength. When Fe(III)-oxide was used as the electron acceptor, fumarate was omitted and a non-chelated mineral mix was used (in which all components of the chelated mix were dissolved in a small volume of 1N HCl without NTA). In all cases, the pH of the medium was adjusted to 6.8, buffered with 2 g/L $NaHCO_3$ and purged with N_2:CO_2 gas (80:20) passed over a heated copper column to remove trace oxygen.

Three-electrode bioreactors were assembled as previously described (60). Briefly, graphite electrodes were polished using 1,500 grit wet/dry sandpaper and attached to platinum wire to serve as the working electrode. A bare platinum wire was the counter electrode. The potential of the working electrode was maintained at -0.10 V vs. standard hydrogen electrode (SHE) using a saturated calomel reference electrode and a VMP3 multichannel potentiostat (Biologic). Reactor headspace was degassed using 80:20 N_2:CO_2 prior to inoculation. Current was measured as an average over two minutes. For all pure culture mutant experiments, a 25% inoculum with cultures reaching acceptor limitation (OD_{600}=0.50-0.55) was used. The total volume of each reactor was 15 ml, and the working electrode surface area was 3 cm^2.

506 To assay Fe(III) oxide reduction in *G. sulfurreducens*, late exponential growth phase cultures
507 (OD_{600} = 0.5-0.55) grown using acetate-fumarate were used to inoculate 1:100 in minimal
508 medium containing 20 mM acetate as the electron donor and 55 mM freshly precipitated β-
509 FeO(OH) as the sole electron acceptor. A small sample of the medium was removed at regular
510 intervals and dissolved in 0.5 N HCl for at least 24 hours in the dark. The acid extractable Fe(II)
511 was measured using a modified FerroZine assay (59).
512 *Escherichia coli* was cultivated in lysogeny broth supplemented with 0.3 M 2,3-diaminopimelic
513 acid and 50 µg/ml kanamycin when needed.
514
515 **Tn-Seq library construction**. Five ml of mid-log (OD_{600} ~0.35) *G. sulfurreducens* culture grown
516 on acetate-fumarate was combined with 5 ml of an overnight culture of *E. coli* conjugative donor
517 strain BW29427 (WM3064) carrying the transposon plasmid pEB001 was applied to a
518 nitrocellulose filter (0.4 µm pore size) using a vacuum. Plasmid pEB001 contains the *mariner*
519 derivative *Himar1* transposon with MmeI recognition sites on both sides of the inverted repeats
520 that flank a kanamycin resistance cassette. *G. sulfurreducens* recipient and *E. coli* donor
521 mixture was washed on the filter with 3 volumes of basal medium before transferring the filter
522 with the cell mixture to an agar plate containing acetate-fumarate and incubated in a Coy
523 chamber at 30°C for 4 hours. The cell mixture was washed off the filter disc with 1 ml of basal
524 medium supplemented with 200 µg/ml kanamycin. To select for *G. sulfurreducens* transposon
525 mutants, dilutions were plated on large 22 x 22 cm square agar plates with acetate-fumarate
526 medium supplemented with kanamycin and incubated at 30°C in the anoxic chamber until
527 visible colonies formed (in six days). Approximately 50,000 colonies were pooled in 10 ml of
528 acetate-fumarate medium and grown for 4 hours before freezing 1 ml aliquots in 10% DMSO.
529
530 **Tn-Seq experiment.** For each experiment, a frozen library aliquot was used to inoculate 100 ml
531 of acetate-fumarate medium. When cultures reached exponential growth phase (OD_{600} ~0.35), 5

ml of this culture was inoculated into fresh 100 ml acetate-fumarate medium. This parent culture was grown to early stationary phase (OD_{600} ~0.5) and used to initiate both electrode and fumarate control experiments. Five ml of the parent culture was inoculated into 100 ml of acetate-fumarate medium and allowed to grow for 6 generations before harvesting. At the same time, a 7.5 ml of the parent culture was inoculated into the 3-electrode bioreactor containing 7.5 ml of medium, where two 3 cm^2 working electrodes were present to support biofilm growth. *G. sulfurreducens* electrode biofilms were harvested by moving reactors to an anaerobic chamber after 6 generations of growth using electrodes poised at -0.1 V SHE, with the number of generations estimated based on the doubling time (10 h) at this redox potential. The entire electrode plus attached biofilm was placed in 100 ml of acetate-fumarate minimal medium, vortexed to liberate cells, and incubated at 30°C for 6 generations before harvesting. This outgrowth was necessary to produce adequate free biomass for DNA extraction and sequencing, and is why cells grown with fumarate for an additional 6 generations were used as a parallel control. Despite this additional outgrowth step, read densities and phenotypes between replicate experiments were highly repeatable (see Fig 1B).

Genomic DNA from 40 ml of cells was isolated using the Wizard genomic DNA purification kit (Promega). The protocol for preparing the DNA library for Illumina sequencing is outlined with modifications (61). Six µg of gDNA was digested with MmeI (New England Biolabs) for 2 hours at 37°C. To this reaction, Antarctic phosphatase (New England Biolabs) was added and incubated at 37°C for an additional hour. Enzymes were inactivated at 65°C for 15 minutes, followed by phenol/chloroform/isoamyl acetate (25:24:1) extraction and ethanol precipitation at -20°C overnight. MmeI digested gDNA and Illumina barcoded adaptor with two random base pair overhangs were ligated using T4 DNA ligase (Epicentre) for 1 hour at 25°C. The transposon with 20 bp of genomic DNA sequence junction and ligated adaptor was amplified using Phusion High GC master mix (New England Biolabs) using primers (P1 M6 MmeI and Gex PCR Primer

2) that anneal to the inverted repeat of the transposon and the ligated Illumina adaptor. The PCR reaction was terminated during linear amplification (24). The 120 bp product was gel purified and saved at -20°C. After Sanger sequencing verification using primer Gex PCR Primer 2 for the presence of the unique barcode, the PCR product was sequenced using Illumina (HiSeq 2500 Rapid chemistry single read 50 bp). Three samples with unique barcodes were mixed in a single Illumina lane generating ~30 M quality-passing reads per sample. All sequencing was performed by the University of Minnesota Genomics Center. Primers and barcoded adaptors used in the construction of the Tn-Seq library are referenced here (61).

Mapping of transposon insertions: For each Tn-Seq library, raw sequences were de-multiplexed and extracted according to the unique barcode. The barcode and transposon sequences were trimmed, keeping only genome sequences that were at least 16 bp in length. Reads were then aligned to our *G. sulfurreducens* reference genome (59) using Bowtie (62) (Version 1.1.2) with no mismatches allowed, and discarding reads that could map in more than one location. In a typical experiment, more that 90% of reads were mapped to unique sites. After subtracting TA insertion sites in genes found to be essential under our conditions, the *G. sulfurreducens* genome contains about 55,000 sites where the *mariner* transposon could insert and produce viable mutants. As we also discounted insertions in the first 5% of a feature, as these often do not produce a knockout phenotype (27), libraries recovered insertions in over 64% of available genomic TA sites that could produce viable mutants, providing an average of nearly 10 independent mutants per gene feature.

Approximately 2.7% of the insertional reads mapped to more than one location in the *G. sulfurreducens* genome due to redundancies. Of interest to our analysis, the *omcB* (GSU2738 – GSU2737) and *omcC* (GSU2735 – GSU2731) gene clusters are tandemly duplicated in the genome. Two genes in each cluster are 99-100% identical (GSU2739-8 and GSU2733-2) at the

584 nucleotide level, preventing unique readsmapping to these genes, while the 12-heme
585 cytochrome genes *omcB* (GSU2737) and *omcC* (GSU2731) share 87% DNA sequence identity
586 and contained a few characteristic sites. When the 20 bp MmeI-generated genomic DNA reads
587 mapped ambiguously to more than one site, they were excluded from analysis, and genes
588 containing such sites were flagged to account for possible “low insertion density” in the gene
589 that would wrongly code it as essential. Similar issues limited the amount of useful data for the
590 small triheme cytochromes encoded in *ppcA-E* because there are few unique 20 bp regions in
591 these small genes adjacent to TA sites. However, most ambiguous reads mapped to the 35
592 transposable elements and duplicated ribosomal RNA genes. All ambiguous mappings were
593 excluded from the essentiality analysis, but were included for total read normalization between
594 barcoded libraries.
595
596 To estimate the severity of a phenotype, the effective change in doubling times for Tn-Seq
597 mutants was calculated. The exponential growth equation was applied using the WT doubling
598 time of 10 hours for the duration of electrode growth (72 hours), comparing the reads in a gene
599 between electrode and fumarate conditions where x is the apparent electrode growth doubling
600 time (hours). According to the conditions of the experiment, a Log_2 ration of -2 after 72 hours
601 implies a mutant with a doubling time of ~15 hours.

$$\frac{Reads(electrode)}{Reads(parent)} = \frac{e^{\frac{ln(2)}{x}*72}}{e^{\frac{ln(2)}{10}*72}}$$

602 All of the Tn-Seq library sequence manipulations were performed in a Galaxy server hosted on
603 the Minnesota Supercomputing Institute at the University of Minnesota (63).
604
605 **Scarless gene deletion in *G. sulfurreducens*.** Roughly 1 kb flanking the targeted gene(s) of
606 interest were cloned into the *sacB* encoding pK18mobsacB plasmid. To prevent disruption of

607 the flanking genes, about 30 bp of the target gene sequence coding for a small peptide was
608 cloned within the flanking region. The *sacB* plasmid was transformed into *E. coli* conjugative
609 donor strain S17-1 to conjugate into *G. sulfurreducens* recipient. One ml of fully grown *G.*
610 *sulfurreducens* acetate-fumarate culture was pelleted on top of 1 ml of S17-1 culture carrying
611 the *sacB* plasmid, mixed on top of a 0.22 µm filter resting on acetate-fumarate agar plates in an
612 anaerobic chamber and incubated for 4 hours before streaking the mixture onto acetate-
613 fumarate plates with 200 µg/ml kanamycin. This procedure selected *G. sulfurreducens* culture
614 with pK18mobsacB integrated into either flanking region of the gene since the plasmid cannot
615 replicate in *G. sulfurreducens*. Scarless gene deletion mutant was selected on acetate-fumarate
616 plates containing 10% sucrose and confirmed using PCR with primers flanking the deletion site
617 (59). The primers used to clone the flanking regions into pK18mobsacB and flanking primers to
618 confirm gene deletions are listed in Table S1.
619
620 **Tn-Seq raw sequencing data**. Illumina sequence data trimmed to remove transposon
621 sequences and barcode sequences, containing only genomic DNA (.fastq) from each condition
622 are deposited in NCBI short read archives with the following accession number: SRX2199236
623 (fumarate outgrowth, used for determining essentiality), SRX2199234 (parent library, used as
624 the reference to compare between fumarate and electrode conditions), and SRX2199233
625 (concatenated with fastq headers HJHKHADXX and HJF5FADXX for electrode outgrowth
626 replicates). Mapping files (.bam) for the fumarate outgrowth dataset used to determine
627 essentiality is deposited as SRX2199235. The reference *G. sulfurreducens* genome used for all
628 mapping was re-sequenced and deposited as SRX1101230. Instructions to view read mapping
629 against our reference genome using IGV is available in supplemental file S7.
630
631
632

Acknowledgements

We thank M. Mehta for initiating the construction and analysis of preliminary Tn-Seq experiments in *G. sulfurreducens.* We thank J. Badalamenti for sequence analysis assistance and data management.

Funding information

This study was supported by grants N000141210308 and N000141612194 from the Office of Naval Research. F. Jimenez-Otero was supported by the Mexican National Council for Science and Technology C.E. Levar was supported by the State of Minnesota-University of Minnesota MNDrive program.

References

1. **Nealson KH**, **Saffarini D**. 1994. Iron and manganese in anaerobic respiration: environmental significance, physiology, and regulation. Annu Rev Microbiol **48**:311–343.

2. **Richter K**, **Schicklberger M**, **Gescher J**. 2012. Dissimilatory reduction of extracellular electron acceptors in anaerobic respiration. Appl Environ Microbiol **78**:913–921.

3. **Bond DR**, **Lovley DR**. 2003. Electricity production by *Geobacter sulfurreducens* attached to electrodes. Appl Environ Microbiol **69**:1548–1555.

4. **Wrighton KC**, **Thrash JC**, **Melnyk RA**, **Bigi JP**, **Byrne-Bailey KG**, **Remis JP**, **Schichnes D**, **Auer M**, **Chang CJ**, **Coates JD**. 2011. Evidence for direct electron transfer by a Gram-positive bacterium isolated from a microbial fuel cell. Appl Environ Microbiol **77**:7633–7639.

5. **Rotaru A-E**, **Shrestha PM**, **Liu F**, **Shrestha M**, **Shrestha D**, **Embree M**, **Zengler K**, **Wardman C**, **Nevin KP**, **Lovley DR**. 2013. A new model for electron flow during anaerobic digestion: direct interspecies electron transfer to *Methanosaeta* for the reduction of carbon dioxide to methane. Energy Environ Sci **7**:408–415.

6. **Rotaru A-E**, **Shrestha PM**, **Liu F**, **Markovaite B**, **Chen S**, **Nevin KP**, **Lovley DR**. 2014. Direct interspecies electron transfer between *Geobacter metallireducens* and *Methanosarcina barkeri*. Appl Environ Microbiol **80**:4599–4605.

7. **Breuer M**, **Rosso KM**, **Blumberger J**, **Butt JN**. 2015. Multi-haem cytochromes in *Shewanella oneidensis* MR-1: structures, functions and opportunities. J R Soc Interface **12**:20141117.

668 8. **Coursolle D**, **Baron DB**, **Bond DR**, **Gralnick JA**. 2010. The Mtr respiratory pathway is
669 essential for reducing flavins and electrodes in *Shewanella oneidensis*. J Bacteriol
670 **192**:467–474.

671 9. **Zacharoff L**, **Chan CH**, **Bond DR**. 2016. Reduction of low potential electron acceptors
672 requires the CbcL inner membrane cytochrome of *Geobacter sulfurreducens*.
673 Bioelectrochemistry Amst Neth **107**:7–13.

674 10. **Levar CE**, **Chan CH**, **Mehta-Kolte MG**, **Bond DR**. 2014. An inner membrane cytochrome
675 required only for reduction of high redox potential extracellular electron acceptors. mBio
676 **5**:e02034-14.

677 11. **Morgado L**, **Bruix M**, **Pessanha M**, **Londer YY**, **Salgueiro CA**. 2010. Thermodynamic
678 characterization of a triheme cytochrome family from *Geobacter sulfurreducens* reveals
679 mechanistic and functional diversity. Biophys J **99**:293–301.

680 12. **Liu Y**, **Wang Z**, **Liu J**, **Levar C**, **Edwards MJ**, **Babauta JT**, **Kennedy DW**, **Shi Z**, **Beyenal**
681 **H**, **Bond DR**, **Clarke TA**, **Butt JN**, **Richardson DJ**, **Rosso KM**, **Zachara JM**,
682 **Fredrickson JK**, **Shi L**. 2014. A trans-outer membrane porin-cytochrome protein complex
683 for extracellular electron transfer by *Geobacter sulfurreducens* PCA. Environ Microbiol Rep
684 **6**:776–785.

685 13. **Liu Y**, **Fredrickson JK**, **Zachara JM**, **Shi L**. 2015. Direct involvement of *ombB*, *omaB*,
686 and *omcB* genes in extracellular reduction of Fe(III) by *Geobacter sulfurreducens* PCA.
687 Front Microbiol **6**.

688 14. **Rollefson JB**, **Stephen CS**, **Tien M**, **Bond DR**. 2011. Identification of an extracellular
689 polysaccharide network essential for cytochrome anchoring and biofilm formation in
690 *Geobacter sulfurreducens*. J Bacteriol **193**:1023–1033.

691 15. **Mehta T**, **Coppi MV**, **Childers SE**, **Lovley DR**. 2005. Outer membrane *c*-type
692 cytochromes required for Fe(III) and Mn(IV) oxide reduction in *Geobacter sulfurreducens*.
693 Appl Environ Microbiol **71**:8634–8641.

694 16. **Reguera G**, **Pollina RB**, **Nicoll JS**, **Lovley DR**. 2007. Possible nonconductive role of
695 *Geobacter sulfurreducens* pilus nanowires in biofilm formation. J Bacteriol **189**:2125–2127.

696 17. **Leang C**, **Coppi MV**, **Lovley DR**. 2003. OmcB, a *c*-type polyheme cytochrome, involved in
697 Fe(III) reduction in *Geobacter sulfurreducens*. J Bacteriol **185**:2096–2103.

698 18. **Leang C**, **Lovley DR**. 2005. Regulation of two highly similar genes, *omcB* and *omcC*, in a
699 10 kb chromosomal duplication in *Geobacter sulfurreducens*. Microbiology **151**:1761–
700 1767.

701 19. **Barquist L**, **Boinett CJ**, **Cain AK**. 2013. Approaches to querying bacterial genomes with
702 transposon-insertion sequencing. RNA Biol **10**:1161–1169.

703 20. **Sarmiento F**, **Mrázek J**, **Whitman WB**. 2013. Genome-scale analysis of gene function in
704 the hydrogenotrophic methanogenic archaeon *Methanococcus maripaludis*. Proc Natl
705 Acad Sci U S A **110**:4726–4731.

706 21. **Pechter KB**, **Gallagher L**, **Pyles H**, **Manoil CS**, **Harwood CS**. 2016. Essential genome of
707 the metabolically versatile Alphaproteobacterium *Rhodopseudomonas palustris*. J Bacteriol
708 **198**:867–876.

709 22. **Brutinel ED**, **Gralnick JA**. 2012. Anomalies of the anaerobic tricarboxylic acid cycle in
710 *Shewanella oneidensis* revealed by Tn-seq. Mol Microbiol **86**:273–283.

711 23. **Bouhenni R**, **Gehrke A**, **Saffarini D**. 2005. Identification of genes involved in cytochrome
712 *c* biogenesis in *Shewanella oneidensis*, using a modified *mariner* transposon. Appl Environ
713 Microbiol **71**:4935–4937.

714 24. **van Opijnen T**, **Bodi KL**, **Camilli A**. 2009. Tn-seq: high-throughput parallel sequencing for
715 fitness and genetic interaction studies in microorganisms. Nat Methods **6**:767–772.

716 25. **Lampe DJ**, **Grant TE**, **Robertson HM**. 1998. Factors affecting transposition of the *Himar1*
717 *mariner* transposon *in vitro*. Genetics **149**:179–187.

718 26. **Mahadevan R**, **Bond DR**, **Butler JE**, **Esteve-Nuñez A**, **Coppi MV**, **Palsson BO**,
719 **Schilling CH**, **Lovley DR**. 2006. Characterization of metabolism in the Fe(III)-reducing
720 organism *Geobacter sulfurreducens* by constraint-based modeling. Appl Environ Microbiol
721 **72**:1558–1568.

722 27. **Yang H**, **Krumholz EW**, **Brutinel ED**, **Palani NP**, **Sadowsky MJ**, **Odlyzko AM**, **Gralnick**
723 **JA**, **Libourel IGL**. 2014. Genome-scale metabolic network validation of *Shewanella*
724 *oneidensis* using transposon insertion frequency analysis. PLoS Comput Biol **10**.

725 28. **Spero MA**, **Aylward FO**, **Currie CR**, **Donohue TJ**. 2015. Phylogenomic analysis and
726 predicted physiological role of the proton-translocating NADH:quinone oxidoreductase
727 (complex I) across bacteria. mBio **6**:389–15.

728 29. **Chowdhury NP**, **Kahnt J**, **Buckel W**. 2015. Reduction of ferredoxin or oxygen by flavin-
729 based electron bifurcation in *Megasphaera elsdenii*. FEBS J **282**:3149–3160.

730 30. **Kim B-C**, **Postier BL**, **Didonato RJ**, **Chaudhuri SK**, **Nevin KP**, **Lovley DR**. 2008.
731 Insights into genes involved in electricity generation in *Geobacter sulfurreducens* via whole

genome microarray analysis of the OmcF-deficient mutant. Bioelectrochemistry Amst Neth **73**:70–75.

31. **Holmes DE**, **Chaudhuri SK**, **Nevin KP**, **Mehta T**, **Methé BA**, **Liu A**, **Ward JE**, **Woodard TL**, **Webster J**, **Lovley DR**. 2006. Microarray and genetic analysis of electron transfer to electrodes in *Geobacter sulfurreducens*. Environ Microbiol **8**:1805–1815.

32. **Majzlan J**, **Navrotsky A**, **Schwertmann U**. 2004. Thermodynamics of iron oxides: Part III. Enthalpies of formation and stability of ferrihydrite (~Fe(OH)3), schwertmannite (~FeO(OH)3/4(SO4)1/8), and ε-Fe2O3 1. Geochim Cosmochim Acta **68**:1049–1059.

33. **Speers A**, **Schindler BD**, **Hwang J**, **Genc A**, **Reguera G**. 2016. Genetic identification of a PilT motor in *Geobacter sulfurreducens* reveals a role for pilus retraction in extracellular electron transfer. Microb Physiol Metab **7**:1578.

34. **Tran HT**, **Krushkal J**, **Antommattei FM**, **Lovley DR**, **Weis RM**. 2008. Comparative genomics of *Geobacter* chemotaxis genes reveals diverse signaling function. BMC Genomics **9**:471.

35. **Porter SL**, **Wadhams GH**, **Armitage JP**. 2011. Signal processing in complex chemotaxis pathways. Nat Rev Microbiol **9**:153–165.

36. **Zou SB**, **Hersch SJ**, **Roy H**, **Wiggers JB**, **Leung AS**, **Buranyi S**, **Xie JL**, **Dare K**, **Ibba M**, **Navarre WW**. 2012. Loss of elongation factor P disrupts bacterial outer membrane integrity. J Bacteriol **194**:413–425.

37. **Lassak J**, **Wilson DN**, **Jung K**. 2016. Stall no more at polyproline stretches with the translation elongation factors EF-P and IF-5A. Mol Microbiol **99**:219–235.

753 38. **Nevin KP**, **Kim B-C**, **Glaven RH**, **Johnson JP**, **Woodard TL**, **Methé BA**, **Didonato RJ**,
754 **Covalla SF**, **Franks AE**, **Liu A**, **Lovley DR**. 2009. Anode biofilm transcriptomics reveals
755 outer surface components essential for high density current production in *Geobacter*
756 *sulfurreducens* fuel cells. PloS One **4**:e5628.

757 39. **Inoue K**, **Leang C**, **Franks AE**, **Woodard TL**, **Nevin KP**, **Lovley DR**. 2011. Specific
758 localization of the *c*-type cytochrome OmcZ at the anode surface in current-producing
759 biofilms of *Geobacter sulfurreducens*. Environ Microbiol Rep **3**:211–217.

760 40. **Summers ZM**, **Fogarty HE**, **Leang C**, **Franks AE**, **Malvankar NS**, **Lovley DR**. 2010.
761 Direct exchange of electrons within aggregates of an evolved syntrophic coculture of
762 anaerobic bacteria. Science **330**:1413–1415.

763 41. **Galushko AS**, **Schink B**. 2000. Oxidation of acetate through reactions of the citric acid
764 cycle by *Geobacter sulfurreducens* in pure culture and in syntrophic coculture. Arch
765 Microbiol **174**:314–321.

766 42. **Ducret A**, **Fleuchot B**, **Bergam P**, **Mignot T**. 2013. Direct live imaging of cell-cell protein
767 transfer by transient outer membrane fusion in *Myxococcus xanthus*. eLife **2**:e00868.

768 43. **Cordero OX**, **Ventouras L-A**, **DeLong EF**, **Polz MF**. 2012. Public good dynamics drive
769 evolution of iron acquisition strategies in natural bacterioplankton populations. Proc Natl
770 Acad Sci U S A **109**:20059–20064.

771 44. **Richter H**, **Nevin KP**, **Jia H**, **Lowy DA**, **Lovley DR**, **Tender LM**. 2009. Cyclic voltammetry
772 of biofilms of wild type and mutant *Geobacter sulfurreducens* on fuel cell anodes indicates
773 possible roles of OmcB, OmcZ, type IV pili, and protons in extracellular electron transfer.
774 Energy Environ Sci **2**:506–516.

775 45. **Hallberg ZF**, **Wang XC**, **Wright TA**, **Nan B**, **Ad O**, **Yeo J**, **Hammond MC**. 2016. Hybrid
776 promiscuous (Hypr) GGDEF enzymes produce cyclic AMP-GMP (3', 3'-cGAMP). Proc Natl
777 Acad Sci U S A **113**:1790–1795.

778 46. **Römling U**, **Galperin MY**, **Gomelsky M**. 2013. Cyclic di-GMP: the first 25 years of a
779 universal bacterial second messenger. Microbiol Mol Biol Rev **77**:1–52.

780 47. **Ding Y-HR**, **Hixson KK**, **Giometti CS**, **Stanley A**, **Esteve-Núñez A**, **Khare T**, **Tollaksen**
781 **SL**, **Zhu W**, **Adkins JN**, **Lipton MS**, **Smith RD**, **Mester T**, **Lovley DR**. 2006. The
782 proteome of dissimilatory metal-reducing microorganism *Geobacter sulfurreducens* under
783 various growth conditions. Biochim Biophys Acta **1764**:1198–1206.

784 48. **Franks AE**, **Nevin KP**, **Glaven RH**, **Lovley DR**. 2010. Microtoming coupled to microarray
785 analysis to evaluate the spatial metabolic status of *Geobacter sulfurreducens* biofilms.
786 ISME J **4**:509–519.

787 49. **Segura D**, **Mahadevan R**, **Juárez K**, **Lovley DR**. 2008. Computational and experimental
788 analysis of redundancy in the central metabolism of*Geobacter sulfurreducens*. PLoS
789 Comput Biol **4**.

790 50. **Rotaru A-E**, **Woodard TL**, **Nevin KP**, **Lovley DR**. 2015. Link between capacity for current
791 production and syntrophic growth in *Geobacter* species. Front Microbiol **6**.

792 51. **Miceli JF**, **Parameswaran P**, **Kang D-W**, **Krajmalnik-Brown R**, **Torres CI**. 2012.
793 Enrichment and analysis of anode-respiring bacteria from diverse anaerobic inocula.
794 Environ Sci Technol **46**:10349–10355.

795 52. **Yokoyama H**, **Ishida M**, **Yamashita T**. 2016. Comparison of anodic community in
796 microbial fuel cells with iron oxide-reducing community. J Microbiol Biotechnol **26**:757–762.

797 53. **Kato S**, **Hashimoto K**, **Watanabe K**. 2012. Methanogenesis facilitated by electric
798 syntrophy via (semi)conductive iron-oxide minerals. Environ Microbiol **14**:1646–1654.

799 54. **Levar CE**, **Rollefson JB**, **Bond DR**. 2013. Energetic and molecular constraints on the
800 mechanism of environmental Fe(III) reduction by *Geobacter*, p. 29–48. *In* Gescher, J,
801 Kappler, A (eds.), Microbial Metal Respiration. Springer Berlin Heidelberg.

802 55. **Le Goff A**, **Holzinger M**, **Cosnier S**. 2015. Recent progress in oxygen-reducing laccase
803 biocathodes for enzymatic biofuel cells. Cell Mol Life Sci CMLS **72**:941–952.

804 56. **Foley JM**, **Rozendal RA**, **Hertle CK**, **Lant PA**, **Rabaey K**. 2010. Life cycle assessment of
805 high-rate anaerobic treatment, microbial fuel cells, and microbial electrolysis cells. Environ
806 Sci Technol **44**:3629–3637.

807 57. **Clauwaert P**, **Aelterman P**, **Pham TH**, **De Schamphelaire L**, **Carballa M**, **Rabaey K**,
808 **Verstraete W**. 2008. Minimizing losses in bio-electrochemical systems: the road to
809 applications. Appl Microbiol Biotechnol **79**:901–913.

810 58. **Logan BE**, **Rabaey K**. 2012. Conversion of wastes into bioelectricity and chemicals by
811 using microbial electrochemical technologies. Science **337**:686–690.

812 59. **Chan CH**, **Levar CE**, **Zacharoff L**, **Badalamenti JP**, **Bond DR**. 2015. Scarless genome
813 editing and stable inducible expression vectors for *Geobacter sulfurreducens*. Appl Environ
814 Microbiol **81**:7178–7186.

815 60. **Marsili E**, **Rollefson JB**, **Baron DB**, **Hozalski RM**, **Bond DR**. 2008. Microbial biofilm
816 voltammetry: direct electrochemical characterization of catalytic electrode-attached
817 biofilms. Appl Environ Microbiol **74**:7329–7337.

818 61. **van Opijnen T**, **Camilli A**. 2010. Genome-wide fitness and genetic interactions
819 determined by Tn-seq, a high-throughput massively parallel sequencing method for
820 microorganisms. Curr Protoc Microbiol 19:E:1E.3:1E.3.1–1E.3.16.

821 62. **Langmead B**, **Trapnell C**, **Pop M**, **Salzberg SL**. 2009. Ultrafast and memory-efficient
822 alignment of short DNA sequences to the human genome. Genome Biol **10**:R25.

823 63. **Afgan E**, **Baker D**, **van den Beek M**, **Blankenberg D**, **Bouvier D**, **Čech M**, **Chilton J**,
824 **Clements D**, **Coraor N**, **Eberhard C**, **Grüning B**, **Guerler A**, **Hillman-Jackson J**, **Von**
825 **Kuster G**, **Rasche E**, **Soranzo N**, **Turaga N**, **Taylor J**, **Nekrutenko A**, **Goecks J**. 2016.
826 The Galaxy platform for accessible, reproducible and collaborative biomedical analyses:
827 2016 update. Nucleic Acids Res **44**:W3–W10.

828 64. **Simon R**, **Priefer U**, **Pühler A**. 1983. A broad host range mobilization system for *in vivo*
829 genetic engineering: transposon mutagenesis in Gram negative bacteria. Nat Biotechnol
830 **1**:784–791.

831
832
833
834
835
836
837
838
839
840
841

842 **Figure Legends**

843

844 **Figure 1. Tn-Seq reproducibility within library replicates and between experimental**
845 **replicates in *Geobacter sulfurreducens*.** (A) Comparison of two subsamples of the same
846 fumarate-grown library. The number of reads mapped to a gene (normalized for read depth) is
847 plotted against data for the same gene prepared and sequenced in parallel. (B) Comparison of
848 two separate cultures inoculated on a poised electrode as terminal electron acceptor, recovered
849 and sequenced separately.

850

851 **Figure 2. Estimation of essential genes based on low insertion densities, and use of *in***
852 ***silico* model data to verify essentiality predictions.** (A) The frequency distribution for
853 fumarate-grown cells follows a bimodal distribution centered around 10 insertions/kb, with
854 strong enrichment below 4 insertions per kb (left of the dashed line). Genes with few insertions
855 are predicted to be essential under these conditions. (B) Most genes labeled as essential in *in*
856 *silico* modeling also contained less than 4 insertion sites per kb, and had less than 300 mapped
857 reads/gene (26).

858

859 **Figure 3. Genes essential for growth with electrodes are not required for Fe(III) reduction.**
860 Growth of scarless deletion mutants of chemosensory-like genes *esnA*, *esnB*, *esnC* and *esnD*
861 and extracellular conduit clusters *extABCD*, *omcBC*, *extEFG* and *extHIJKL* with (A) insoluble
862 Fe(III) oxides and (B) poised electrodes. The amount of Fe(III) reduced in 7 days was
863 normalized to WT. Maximum current densities on electrodes poised at -0.1 V vs. SHE were
864 recorded for all strains 80 hours after inoculation. All experiments were performed in triplicate.

865

866

867

Table 1. Strains and plasmids used in this work

Strain or Plasmid	Description or relevant genotype	Source or reference
G. sulfurreducens strains		
DB823	Δ*esnA* (ΔGSU1704)	This study
DB836	Δ*esnB* (ΔGSU2220)	This study
DB824	Δ*esnC* (ΔGSU2222)	This study
DB1130	Δ*esnD* (ΔGSU3376)	This study
DB1280	Δ*extABCD* (ΔGSU2645-GSU2642)	This study
DB1282	Δ*extEFG* (ΔGSU2726-GSU2724)	This study
DB1279	Δ*omcBC* cluster (ΔGSU2739-GSU2731)	This study
DB1281	Δ*extHIJKL* (ΔGSU2940-GSU2936)	This study
E. coli strains		
S17-1	*recA pro hsdR RP4-2-Tc*::Mu-Km::Tn*7*	(64)
BW29427 (WM3064)	*thrB1004 pro thi rpsL hsdS lacZ*Δ*M15 RP4-1360* Δ*(araBAD)567* Δ*dapA1341*::[*erm pir*]	K. Datsenko and B. L. Wanner
Plasmids		
pEB001	Plasmid carrying mini*Himar* RB1 transposon with engineered MmeI restriction sites	(22)
pK18mobsacB	SacB encoding scarless deletion vector	(64)
pDGSU1704	Flanking regions of GSU1704 in pK18mobsacB	This study
pDGSU2220	Flanking regions of GSU2220 in pK18mobsacB	This study
pDGSU2222	Flanking regions of GSU2222 in pK18mobsacB	This study
pDGSU3376	Flanking regions of GSU3376 in pK18mobsacB	This study
pDGSU2645-2642	Flanking regions of GSU2645-2642 in pK18mobsacB	This study
pDGSU2726-2724	Flanking regions of GSU2726-2724 in pK18mobsacB	This study
pDGSU2739-2731	Flanking regions of GSU2739-2731 in pK18mobsacB	This study
pDGSU2940-2936	Flanking regions of GSU2940-2936 in pK18mobsacB	This study

887 **Table 2.** TnSeq mutations which after growth on an electrode showed a decrease in reads
888 mapped by at least a Log_2 ratio of -2, equivalent to a predicted 50% reduction in growth rate.
889

Locus	Gene symbol and description	Log_2 ratio
Cytochrome		
GSU0274	*cbcL*, *c*- and *b*-type cytochrome	-3.3
GSU2643	*extC*, lipoprotein cytochrome *c*	-2.0
GSU2645	*extA*, cytochrome *c*	-2.5
Metabolism and protein processing		
GSU0140	phosphoribosylaminoimidazole carboxylase-like protein	-2.2
GSU0503	*crcB*, camphor resistance protein CrcB	-2.2
GSU0536	adenosine nucleotide alpha-hydrolase superfamily protein	-2.6
GSU0994	*fumB*, fumarate hydratase	-8.0
GSU1105	prolidase family protein	-2.0
GSU1279	*nikMN*, nickel ABC transporter membrane protein NikMN	-2.0
GSU1752	*efp-2*, elongation factor P	-2.5
GSU1753	*genX*, translation elongation factor P-lysine lysyltransferase	-2.9
GSU1754	*yjeK*, translation elongation factor P-lysyl-lysine 2,3-aminomutase	-2.8
GSU3278	pentapeptide repeat-containing protein	-2.0
Signaling and regulation		
GSU0013	MarR family winged helix-turn-helix transcriptional regulator	-2.1
GSU1704	*esnA*, GAF sensor methyl-accepting chemotaxis sensory transducer, class 40H	-2.4
GSU2220	*esnB*, scaffold protein CheW associated with MCPs of class 40H	-2.4
GSU2221	ATPase	-2.1
GSU2222	*esnC*, sensor histidine kinase CheA associated with MCPs of class 40H	-2.8[a]
Extracellular structures		
GSU1114	lipoprotein	-2.1
GSU1493	*pilC*, type IV pilus inner membrane protein PilC	-2.2
GSU1494	*pilS*, sensor histidine kinase PilS, PAS domain-containing	-2.2
GSU1501	*xapD*, ABC transporter ATP-binding protein	-2.0
GSU1816	*ugd*, UDP-glucose 6-dehydrogenase	-2.0
GSU1889	*lptA*, lipopolysaccharide ABC transporter periplasmic protein LptA	-6.5
GSU1976	YqgM-like family glycosyltransferase	-4.9
GSU2028	*pilQ*, type IV pilus secretin lipoprotein PilQ	-2.5
GSU2029	*pilP*, type IV pilus assembly lipoprotein PilP	-3.3
GSU2030	*pilO*, type IV pilus biogenesis protein PilO	-2.5
GSU2032	*pilM*, type IV pilus biogenesis ATPase PilM	-2.4
GSU2085	*hldE*, D-glycero-D-mannoheptose-7-phosphate kinase and D-glycero-D-mannoheptose-1-phosphate adenylyltransferase	-3.1
GSU2087	*gmhA*, phosphoheptose isomerase	-3.7
GSU2973	lipoprotein	-2.7
GSU3321	phosphoglucomutase/phosphomannomutase family protein	-2.2
Hypothetical		
GSU2086	hypothetical protein	-3.2
GSU2713	hypothetical protein	-2.9
GSU2257	hypothetical protein	-2.4
GSU0141	hypothetical protein	-2.3
GSU0959	hypothetical protein	-2.3
GSU2048	hypothetical protein	-2.1

890
891 [a] coded as essential in our study
892

Figure 1

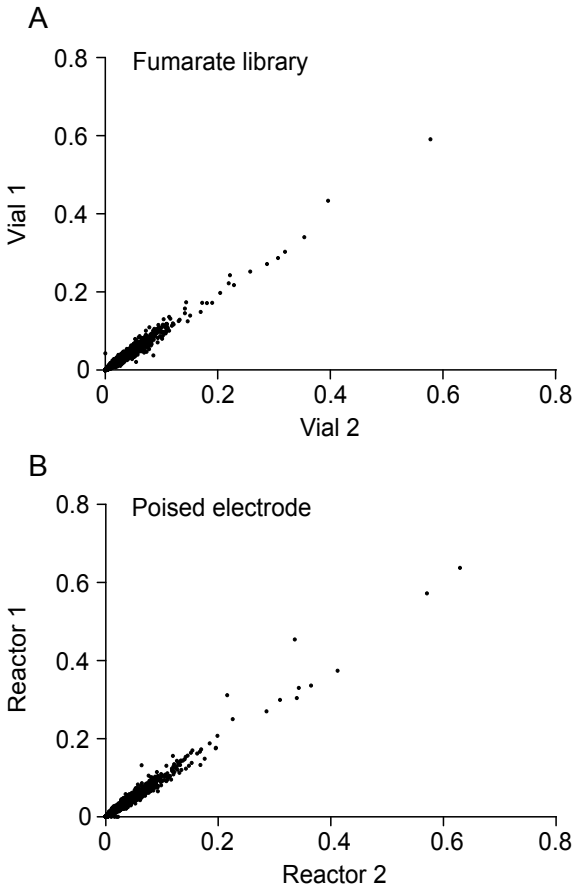

Figure 1. Tn-Seq reproducibility within library replicates and between experimental replicates in *Geobacter sulfurreducens*. (A) Comparison of two subsamples of the same fumarate-grown library. The number of reads mapped to a gene (normalized for read depth) is plotted against data for the same gene prepared and sequenced in parallel. (B) Comparison of two separate cultures inoculated on a poised electrode as terminal electron acceptor, recovered and sequenced separately.

Figure 2

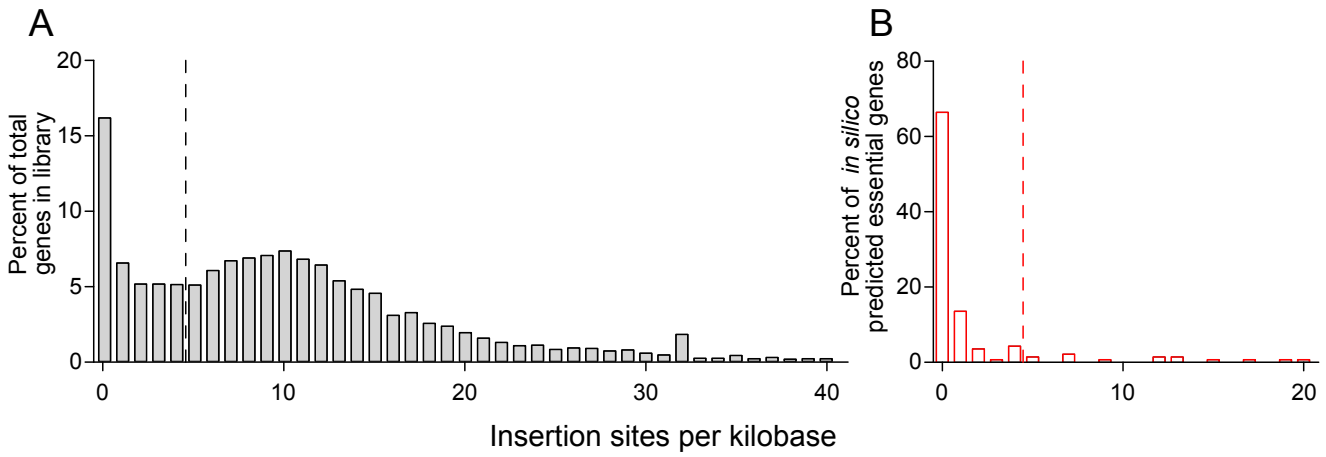

Figure 2. Estimation of essential genes based on low insertion densities, and use of *in silico* model data to verify essentiality predictions. (A) The frequency distribution for fumarate-grown cells follows a bimodal distribution centered around 10 insertions/kb, with strong enrichment below 4 insertions per kb (left of the dashed line). Genes with few insertions are predicted to be essential under these conditions. (B) Most genes labeled as essential in in silico modeling also contained less than 4 insertion sites per kb, and had less than 300 mapped reads/gene (26).

Figure 3

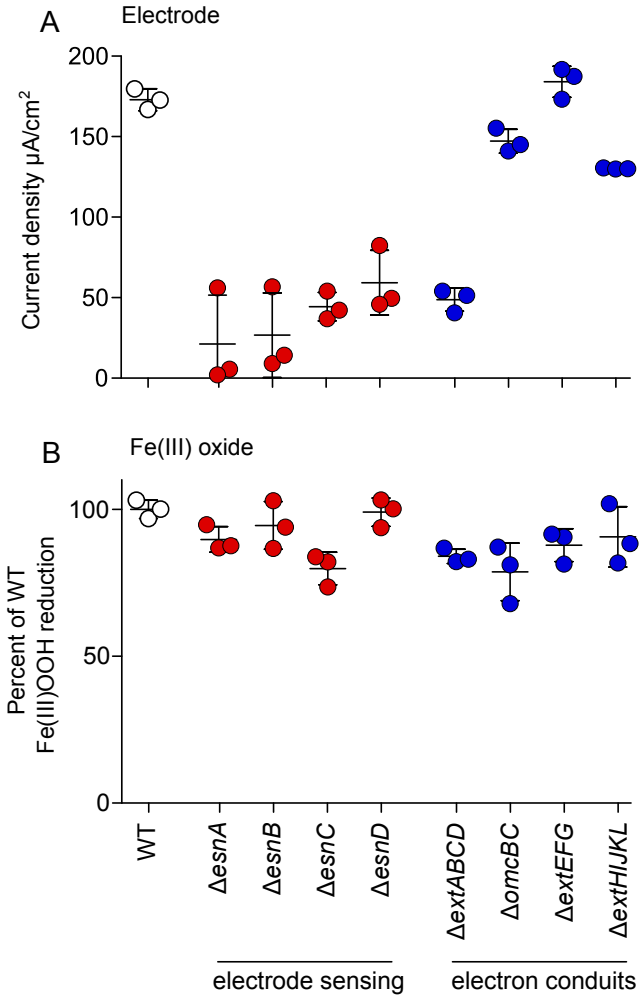

Figure 3. Genes essential for growth with electrodes are not required for Fe(III) reduction. Growth of scarless deletion mutants of chemosensory-like genes *esnA*, *esnB*, *esnC* and *esnD* and extracellular conduit clusters *extABCD*, *omcBC*, *extEFG* and *extHIJKL* with (A) insoluble Fe(III) oxides and (B) poised electrodes. The amount of Fe(III) reduced in 7 days was normalized to WT. Maximum current densities on electrodes poised at -0.1 V vs. SHE were recorded for all strains 80 hours after inoculation. All experiments were performed in triplicate.